

Observation of inclusive $D^{*\pm}$ production in the decay of $\Upsilon(1S)$

B. Aubert,¹ Y. Karyotakis,¹ J. P. Lees,¹ V. Poireau,¹ E. Prencipe,¹ X. Prudent,¹ V. Tisserand,¹ J. Garra Tico,² E. Grauges,² M. Martinelli^{ab,3} A. Palano^{ab,3} M. Pappagallo^{ab,3} G. Eigen,⁴ B. Stugu,⁴ L. Sun,⁴ M. Battaglia,⁵ D. N. Brown,⁵ B. Hooberman,⁵ L. T. Kerth,⁵ Yu. G. Kolomensky,⁵ G. Lynch,⁵ I. L. Osipenko,⁵ K. Tackmann,⁵ T. Tanabe,⁵ C. M. Hawkes,⁶ N. Soni,⁶ A. T. Watson,⁶ H. Koch,⁷ T. Schroeder,⁷ D. J. Asgeirsson,⁸ C. Hearty,⁸ T. S. Mattison,⁸ J. A. McKenna,⁸ M. Barrett,⁹ A. Khan,⁹ A. Randle-Conde,⁹ V. E. Blinov,¹⁰ A. D. Bukin,^{10,*} A. R. Buzykaev,¹⁰ V. P. Druzhinin,¹⁰ V. B. Golubev,¹⁰ A. P. Onuchin,¹⁰ S. I. Serednyakov,¹⁰ Yu. I. Skovpen,¹⁰ E. P. Solodov,¹⁰ K. Yu. Todyshev,¹⁰ M. Bondioli,¹¹ S. Curry,¹¹ I. Eschrich,¹¹ D. Kirkby,¹¹ A. J. Lankford,¹¹ P. Lund,¹¹ M. Mandelkern,¹¹ E. C. Martin,¹¹ D. P. Stoker,¹¹ H. Atmacan,¹² J. W. Gary,¹² F. Liu,¹² O. Long,¹² G. M. Vitug,¹² Z. Yasin,¹² V. Sharma,¹³ C. Campagnari,¹⁴ T. M. Hong,¹⁴ D. Kovalskyi,¹⁴ M. A. Mazur,¹⁴ J. D. Richman,¹⁴ T. W. Beck,¹⁵ A. M. Eisner,¹⁵ C. A. Heusch,¹⁵ J. Kroseberg,¹⁵ W. S. Lockman,¹⁵ A. J. Martinez,¹⁵ T. Schalk,¹⁵ B. A. Schumm,¹⁵ A. Seiden,¹⁵ L. O. Winstrom,¹⁵ C. H. Cheng,¹⁶ D. A. Doll,¹⁶ B. Echenard,¹⁶ F. Fang,¹⁶ D. G. Hitlin,¹⁶ I. Narsky,¹⁶ P. Ongmongkolkul,¹⁶ T. Piatenko,¹⁶ F. C. Porter,¹⁶ R. Andreassen,¹⁷ M. S. Dubrovin,¹⁷ G. Mancinelli,¹⁷ B. T. Meadows,¹⁷ K. Mishra,¹⁷ M. D. Sokoloff,¹⁷ P. C. Bloom,¹⁸ W. T. Ford,¹⁸ A. Gaz,¹⁸ J. F. Hirschauer,¹⁸ M. Nagel,¹⁸ U. Nauenberg,¹⁸ J. G. Smith,¹⁸ S. R. Wagner,¹⁸ R. Ayad,^{19,†} W. H. Toki,¹⁹ E. Feltresi,²⁰ A. Hauke,²⁰ H. Jasper,²⁰ T. M. Karbach,²⁰ J. Merkel,²⁰ A. Petzold,²⁰ B. Spaan,²⁰ K. Wacker,²⁰ M. J. Kobel,²¹ K. R. Schubert,²¹ R. Schwierz,²¹ D. Bernard,²² E. Latour,²² M. Verderi,²² P. J. Clark,²³ S. Playfer,²³ J. E. Watson,²³ M. Andreotti^{ab,24} D. Bettoni^{a,24} C. Bozzi^{a,24} R. Calabrese^{ab,24} A. Cecchi^{ab,24} G. Cibinetto^{ab,24} E. Fioravanti^{ab,24} P. Franchini^{ab,24} E. Luppi^{ab,24} M. Munerato^{ab,24} M. Negrini^{ab,24} A. Petrella^{ab,24} L. Piemontese^{a,24} V. Santoro^{ab,24} R. Baldini-Ferrolì,²⁵ A. Calcaterra,²⁵ R. de Sangro,²⁵ G. Finocchiaro,²⁵ S. Pacetti,²⁵ P. Patteri,²⁵ I. M. Peruzzi,^{25,‡} M. Piccolo,²⁵ M. Rama,²⁵ A. Zallo,²⁵ R. Contri^{ab,26} E. Guido^{ab,26} M. Lo Vetere^{ab,26} M. R. Monge^{ab,26} S. Passaggio^{a,26} C. Patrignani^{ab,26} E. Robutti^{a,26} S. Tosi^{ab,26} M. Morii,²⁷ A. Adametz,²⁸ J. Marks,²⁸ S. Schenk,²⁸ U. Uwer,²⁸ F. U. Bernlochner,²⁹ H. M. Lacker,²⁹ T. Lueck,²⁹ A. Volk,²⁹ P. D. Dauncey,³⁰ M. Tibbetts,³⁰ P. K. Behera,³¹ M. J. Charles,³¹ U. Mallik,³¹ C. Chen,³² J. Cochran,³² H. B. Crawley,³² L. Dong,³² V. Eyges,³² W. T. Meyer,³² S. Prell,³² E. I. Rosenberg,³² A. E. Rubin,³² Y. Y. Gao,³³ A. V. Gritsan,³³ Z. J. Guo,³³ N. Arnaud,³⁴ M. Davier,³⁴ D. Derkach,³⁴ J. Firmino da Costa,³⁴ G. Grosdidier,³⁴ F. Le Diberder,³⁴ V. Lepeltier,³⁴ A. M. Lutz,³⁴ B. Malaescu,³⁴ P. Roudeau,³⁴ M. H. Schune,³⁴ J. Serrano,³⁴ V. Sordini,^{34,§} A. Stocchi,³⁴ G. Wormser,³⁴ D. J. Lange,³⁵ D. M. Wright,³⁵ I. Bingham,³⁶ J. P. Burke,³⁶ C. A. Chavez,³⁶ J. R. Fry,³⁶ E. Gabathuler,³⁶ R. Gamet,³⁶ D. E. Hutchcroft,³⁶ D. J. Payne,³⁶ C. Touramanis,³⁶ A. J. Bevan,³⁷ C. K. Clarke,³⁷ F. Di Lodovico,³⁷ R. Sacco,³⁷ M. Sigamani,³⁷ G. Cowan,³⁸ S. Paramesvaran,³⁸ A. C. Wren,³⁸ D. N. Brown,³⁹ C. L. Davis,³⁹ A. G. Denig,⁴⁰ M. Fritsch,⁴⁰ W. Gradl,⁴⁰ A. Hafner,⁴⁰ K. E. Alwyn,⁴¹ D. Bailey,⁴¹ R. J. Barlow,⁴¹ G. Jackson,⁴¹ G. D. Lafferty,⁴¹ T. J. West,⁴¹ J. I. Yi,⁴¹ J. Anderson,⁴² A. Jawahery,⁴² D. A. Roberts,⁴² G. Simi,⁴² J. M. Tuggle,⁴² C. Dallapiccola,⁴³ E. Salvati,⁴³ R. Cowan,⁴⁴ D. Dujmic,⁴⁴ P. H. Fisher,⁴⁴ S. W. Henderson,⁴⁴ G. Sciolla,⁴⁴ M. Spitznagel,⁴⁴ R. K. Yamamoto,⁴⁴ M. Zhao,⁴⁴ P. M. Patel,⁴⁵ S. H. Robertson,⁴⁵ M. Schram,⁴⁵ P. Biassoni^{ab,46} A. Lazzaro^{ab,46} V. Lombardo^{a,46} F. Palombo^{ab,46} S. Stracka^{ab,46} L. Cremaldi,⁴⁷ R. Godang,^{47,¶} R. Kroeger,⁴⁷ P. Sonnek,⁴⁷ D. J. Summers,⁴⁷ H. W. Zhao,⁴⁷ X. Nguyen,⁴⁸ M. Simard,⁴⁸ P. Taras,⁴⁸ H. Nicholson,⁴⁹ G. De Nardo^{ab,50} L. Lista^{a,50} D. Monorchio^{ab,50} G. Onorato^{ab,50} C. Sciacca^{ab,50} G. Raven,⁵¹ H. L. Snoek,⁵¹ C. P. Jessop,⁵² K. J. Knoepfel,⁵² J. M. LoSecco,⁵² W. F. Wang,⁵² L. A. Corwin,⁵³ K. Honscheid,⁵³ H. Kagan,⁵³ R. Kass,⁵³ J. P. Morris,⁵³ A. M. Rahimi,⁵³ S. J. Sekula,⁵³ N. L. Blount,⁵⁴ J. Brau,⁵⁴ R. Frey,⁵⁴ O. Igonkina,⁵⁴ J. A. Kolb,⁵⁴ M. Lu,⁵⁴ R. Rahmat,⁵⁴ N. B. Sinev,⁵⁴ D. Strom,⁵⁴ J. Strube,⁵⁴ E. Torrence,⁵⁴ G. Castelli^{ab,55} N. Gagliardi^{ab,55} M. Margoni^{ab,55} M. Morandin^{a,55} M. Posocco^{a,55} M. Rotondo^{a,55} F. Simonetto^{ab,55} R. Stroili^{ab,55} C. Voci^{ab,55} P. del Amo Sanchez,⁵⁶ E. Ben-Haim,⁵⁶ G. R. Bonneaud,⁵⁶ H. Briand,⁵⁶ J. Chauveau,⁵⁶ O. Hamon,⁵⁶ Ph. Leruste,⁵⁶ G. Marchiori,⁵⁶ J. Ocariz,⁵⁶ A. Perez,⁵⁶ J. Prendki,⁵⁶ S. Sitt,⁵⁶ L. Gladney,⁵⁷ M. Biasini^{ab,58} E. Manoni^{ab,58} C. Angelini^{ab,59} G. Batignani^{ab,59} S. Bettarini^{ab,59} G. Calderini^{ab,59,**} M. Carpinelli^{ab,59,††} A. Cervelli^{ab,59} F. Forti^{ab,59} M. A. Giorgi^{ab,59} A. Lusiani^{ac,59} M. Morganti^{ab,59} N. Neri^{ab,59} E. Paoloni^{ab,59} G. Rizzo^{ab,59} J. J. Walsh^{a,59} D. Lopes Pegna,⁶⁰ C. Lu,⁶⁰ J. Olsen,⁶⁰ A. J. S. Smith,⁶⁰ A. V. Telnov,⁶⁰ F. Anulli^{a,61} E. Baracchini^{ab,61} G. Cavoto^{a,61} R. Faccini^{ab,61} F. Ferrarotto^{a,61} F. Ferroni^{ab,61} M. Gaspero^{ab,61} P. D. Jackson^{a,61} L. Li Gioi^{a,61} M. A. Mazzoni^{a,61} S. Morganti^{a,61} G. Piredda^{a,61} F. Renga^{ab,61}

C. Voena^{a,61} M. Ebert,⁶² T. Hartmann,⁶² H. Schröder,⁶² R. Waldi,⁶² T. Adye,⁶³ B. Franek,⁶³ E. O. Olaiya,⁶³ F. F. Wilson,⁶³ S. Emery,⁶⁴ L. Esteve,⁶⁴ G. Hamel de Monchenault,⁶⁴ W. Kozanecki,⁶⁴ G. Vasseur,⁶⁴ Ch. Yèche,⁶⁴ M. Zito,⁶⁴ M. T. Allen,⁶⁵ D. Aston,⁶⁵ D. J. Bard,⁶⁵ R. Bartoldus,⁶⁵ J. F. Benitez,⁶⁵ R. Cenci,⁶⁵ J. P. Coleman,⁶⁵ M. R. Convery,⁶⁵ J. C. Dingfelder,⁶⁵ J. Dorfan,⁶⁵ G. P. Dubois-Felsmann,⁶⁵ W. Dunwoodie,⁶⁵ R. C. Field,⁶⁵ M. Franco Sevilla,⁶⁵ B. G. Fulson,⁶⁵ A. M. Gabareen,⁶⁵ M. T. Graham,⁶⁵ P. Grenier,⁶⁵ C. Hast,⁶⁵ W. R. Innes,⁶⁵ J. Kaminski,⁶⁵ M. H. Kelsey,⁶⁵ H. Kim,⁶⁵ P. Kim,⁶⁵ M. L. Kocian,⁶⁵ D. W. G. S. Leith,⁶⁵ S. Li,⁶⁵ B. Lindquist,⁶⁵ S. Luitz,⁶⁵ V. Luth,⁶⁵ H. L. Lynch,⁶⁵ D. B. MacFarlane,⁶⁵ H. Marsiske,⁶⁵ R. Messner,^{65,*} D. R. Muller,⁶⁵ H. Neal,⁶⁵ S. Nelson,⁶⁵ C. P. O'Grady,⁶⁵ I. Ofte,⁶⁵ M. Perl,⁶⁵ B. N. Ratcliff,⁶⁵ A. Roodman,⁶⁵ A. A. Salmikov,⁶⁵ R. H. Schindler,⁶⁵ J. Schwiening,⁶⁵ A. Snyder,⁶⁵ D. Su,⁶⁵ M. K. Sullivan,⁶⁵ K. Suzuki,⁶⁵ S. K. Swain,⁶⁵ J. M. Thompson,⁶⁵ J. Va'vra,⁶⁵ A. P. Wagner,⁶⁵ M. Weaver,⁶⁵ C. A. West,⁶⁵ W. J. Wisniewski,⁶⁵ M. Wittgen,⁶⁵ D. H. Wright,⁶⁵ H. W. Wulsin,⁶⁵ A. K. Yarritu,⁶⁵ C. C. Young,⁶⁵ V. Ziegler,⁶⁵ X. R. Chen,⁶⁶ H. Liu,⁶⁶ W. Park,⁶⁶ M. V. Purohit,⁶⁶ R. M. White,⁶⁶ J. R. Wilson,⁶⁶ M. Bellis,⁶⁷ P. R. Burchat,⁶⁷ A. J. Edwards,⁶⁷ T. S. Miyashita,⁶⁷ S. Ahmed,⁶⁸ M. S. Alam,⁶⁸ J. A. Ernst,⁶⁸ B. Pan,⁶⁸ M. A. Saeed,⁶⁸ S. B. Zain,⁶⁸ A. Soffer,⁶⁹ S. M. Spanier,⁷⁰ B. J. Wogsland,⁷⁰ R. Eckmann,⁷¹ J. L. Ritchie,⁷¹ A. M. Ruland,⁷¹ C. J. Schilling,⁷¹ R. F. Schwitters,⁷¹ B. C. Wray,⁷¹ B. W. Drummond,⁷² J. M. Izen,⁷² X. C. Lou,⁷² F. Bianchi^{ab,73} D. Gamba^{ab,73} M. Pelliccioni^{ab,73} M. Bomben^{ab,74} L. Bosisio^{ab,74} C. Cartaro^{ab,74} G. Della Ricca^{ab,74} L. Lanceri^{ab,74} L. Vitale^{ab,74} V. Azzolini,⁷⁵ N. Lopez-March,⁷⁵ F. Martinez-Vidal,⁷⁵ D. A. Milanese,⁷⁵ A. Oyanguren,⁷⁵ J. Albert,⁷⁶ Sw. Banerjee,⁷⁶ B. Bhuyan,⁷⁶ H. H. F. Choi,⁷⁶ K. Hamano,⁷⁶ G. J. King,⁷⁶ R. Kowalewski,⁷⁶ M. J. Lewczuk,⁷⁶ I. M. Nugent,⁷⁶ J. M. Roney,⁷⁶ R. J. Sobie,⁷⁶ T. J. Gershon,⁷⁷ P. F. Harrison,⁷⁷ J. Ilic,⁷⁷ T. E. Latham,⁷⁷ G. B. Mohanty,⁷⁷ E. M. T. Puccio,⁷⁷ H. R. Band,⁷⁸ X. Chen,⁷⁸ S. Dasu,⁷⁸ K. T. Flood,⁷⁸ Y. Pan,⁷⁸ R. Prepost,⁷⁸ C. O. Vuosalo,⁷⁸ and S. L. Wu⁷⁸

(The BABAR Collaboration)

¹Laboratoire d'Annecy-le-Vieux de Physique des Particules (LAPP),

Université de Savoie, CNRS/IN2P3, F-74941 Annecy-Le-Vieux, France

²Universitat de Barcelona, Facultat de Física, Departament ECM, E-08028 Barcelona, Spain

³INFN Sezione di Bari^a; Dipartimento di Fisica, Università di Bari^b, I-70126 Bari, Italy

⁴University of Bergen, Institute of Physics, N-5007 Bergen, Norway

⁵Lawrence Berkeley National Laboratory and University of California, Berkeley, California 94720, USA

⁶University of Birmingham, Birmingham, B15 2TT, United Kingdom

⁷Ruhr Universität Bochum, Institut für Experimentalphysik 1, D-44780 Bochum, Germany

⁸University of British Columbia, Vancouver, British Columbia, Canada V6T 1Z1

⁹Brunel University, Uxbridge, Middlesex UB8 3PH, United Kingdom

¹⁰Budker Institute of Nuclear Physics, Novosibirsk 630090, Russia

¹¹University of California at Irvine, Irvine, California 92697, USA

¹²University of California at Riverside, Riverside, California 92521, USA

¹³University of California at San Diego, La Jolla, California 92093, USA

¹⁴University of California at Santa Barbara, Santa Barbara, California 93106, USA

¹⁵University of California at Santa Cruz, Institute for Particle Physics, Santa Cruz, California 95064, USA

¹⁶California Institute of Technology, Pasadena, California 91125, USA

¹⁷University of Cincinnati, Cincinnati, Ohio 45221, USA

¹⁸University of Colorado, Boulder, Colorado 80309, USA

¹⁹Colorado State University, Fort Collins, Colorado 80523, USA

²⁰Technische Universität Dortmund, Fakultät Physik, D-44221 Dortmund, Germany

²¹Technische Universität Dresden, Institut für Kern- und Teilchenphysik, D-01062 Dresden, Germany

²²Laboratoire Leprince-Ringuet, CNRS/IN2P3, Ecole Polytechnique, F-91128 Palaiseau, France

²³University of Edinburgh, Edinburgh EH9 3JZ, United Kingdom

²⁴INFN Sezione di Ferrara^a; Dipartimento di Fisica, Università di Ferrara^b, I-44100 Ferrara, Italy

²⁵INFN Laboratori Nazionali di Frascati, I-00044 Frascati, Italy

²⁶INFN Sezione di Genova^a; Dipartimento di Fisica, Università di Genova^b, I-16146 Genova, Italy

²⁷Harvard University, Cambridge, Massachusetts 02138, USA

²⁸Universität Heidelberg, Physikalisches Institut, Philosophenweg 12, D-69120 Heidelberg, Germany

²⁹Humboldt-Universität zu Berlin, Institut für Physik, Newtonstr. 15, D-12489 Berlin, Germany

³⁰Imperial College London, London, SW7 2AZ, United Kingdom

³¹University of Iowa, Iowa City, Iowa 52242, USA

³²Iowa State University, Ames, Iowa 50011-3160, USA

³³Johns Hopkins University, Baltimore, Maryland 21218, USA

³⁴Laboratoire de l'Accélérateur Linéaire, IN2P3/CNRS et Université Paris-Sud 11,

Centre Scientifique d'Orsay, B. P. 34, F-91898 Orsay Cedex, France

³⁵Lawrence Livermore National Laboratory, Livermore, California 94550, USA

³⁶University of Liverpool, Liverpool L69 7ZE, United Kingdom

- ³⁷Queen Mary, University of London, London, E1 4NS, United Kingdom
- ³⁸University of London, Royal Holloway and Bedford New College, Egham, Surrey TW20 0EX, United Kingdom
- ³⁹University of Louisville, Louisville, Kentucky 40292, USA
- ⁴⁰Johannes Gutenberg-Universität Mainz, Institut für Kernphysik, D-55099 Mainz, Germany
- ⁴¹University of Manchester, Manchester M13 9PL, United Kingdom
- ⁴²University of Maryland, College Park, Maryland 20742, USA
- ⁴³University of Massachusetts, Amherst, Massachusetts 01003, USA
- ⁴⁴Massachusetts Institute of Technology, Laboratory for Nuclear Science, Cambridge, Massachusetts 02139, USA
- ⁴⁵McGill University, Montréal, Québec, Canada H3A 2T8
- ⁴⁶INFN Sezione di Milano^a; Dipartimento di Fisica, Università di Milano^b, I-20133 Milano, Italy
- ⁴⁷University of Mississippi, University, Mississippi 38677, USA
- ⁴⁸Université de Montréal, Physique des Particules, Montréal, Québec, Canada H3C 3J7
- ⁴⁹Mount Holyoke College, South Hadley, Massachusetts 01075, USA
- ⁵⁰INFN Sezione di Napoli^a; Dipartimento di Scienze Fisiche, Università di Napoli Federico II^b, I-80126 Napoli, Italy
- ⁵¹NIKHEF, National Institute for Nuclear Physics and High Energy Physics, NL-1009 DB Amsterdam, The Netherlands
- ⁵²University of Notre Dame, Notre Dame, Indiana 46556, USA
- ⁵³Ohio State University, Columbus, Ohio 43210, USA
- ⁵⁴University of Oregon, Eugene, Oregon 97403, USA
- ⁵⁵INFN Sezione di Padova^a; Dipartimento di Fisica, Università di Padova^b, I-35131 Padova, Italy
- ⁵⁶Laboratoire de Physique Nucléaire et de Hautes Energies, IN2P3/CNRS, Université Pierre et Marie Curie-Paris6, Université Denis Diderot-Paris7, F-75252 Paris, France
- ⁵⁷University of Pennsylvania, Philadelphia, Pennsylvania 19104, USA
- ⁵⁸INFN Sezione di Perugia^a; Dipartimento di Fisica, Università di Perugia^b, I-06100 Perugia, Italy
- ⁵⁹INFN Sezione di Pisa^a; Dipartimento di Fisica, Università di Pisa^b; Scuola Normale Superiore di Pisa^c, I-56127 Pisa, Italy
- ⁶⁰Princeton University, Princeton, New Jersey 08544, USA
- ⁶¹INFN Sezione di Roma^a; Dipartimento di Fisica, Università di Roma La Sapienza^b, I-00185 Roma, Italy
- ⁶²Universität Rostock, D-18051 Rostock, Germany
- ⁶³Rutherford Appleton Laboratory, Chilton, Didcot, Oxon, OX11 0QX, United Kingdom
- ⁶⁴CEA, Irfu, SPP, Centre de Saclay, F-91191 Gif-sur-Yvette, France
- ⁶⁵SLAC National Accelerator Laboratory, Stanford, California 94309 USA
- ⁶⁶University of South Carolina, Columbia, South Carolina 29208, USA
- ⁶⁷Stanford University, Stanford, California 94305-4060, USA
- ⁶⁸State University of New York, Albany, New York 12222, USA
- ⁶⁹Tel Aviv University, School of Physics and Astronomy, Tel Aviv, 69978, Israel
- ⁷⁰University of Tennessee, Knoxville, Tennessee 37996, USA
- ⁷¹University of Texas at Austin, Austin, Texas 78712, USA
- ⁷²University of Texas at Dallas, Richardson, Texas 75083, USA
- ⁷³INFN Sezione di Torino^a; Dipartimento di Fisica Sperimentale, Università di Torino^b, I-10125 Torino, Italy
- ⁷⁴INFN Sezione di Trieste^a; Dipartimento di Fisica, Università di Trieste^b, I-34127 Trieste, Italy
- ⁷⁵IFIC, Universitat de Valencia-CSIC, E-46071 Valencia, Spain
- ⁷⁶University of Victoria, Victoria, British Columbia, Canada V8W 3P6
- ⁷⁷Department of Physics, University of Warwick, Coventry CV4 7AL, United Kingdom
- ⁷⁸University of Wisconsin, Madison, Wisconsin 53706, USA

We present a study of the inclusive $D^{*\pm}$ production in the decay of $\Upsilon(1S)$ using $(98.6 \pm 0.9) \times 10^6$ $\Upsilon(2S)$ mesons collected with the BABAR detector at the $\Upsilon(2S)$ resonance. Using the decay chain $\Upsilon(2S) \rightarrow \pi^+\pi^-\Upsilon(1S)$, $\Upsilon(1S) \rightarrow D^{*\pm}X$, where X is unobserved, we measure the branching fraction $\mathcal{B}[\Upsilon(1S) \rightarrow D^{*\pm}X] = (2.52 \pm 0.13(\text{stat}) \pm 0.15(\text{syst}))\%$ and the $D^{*\pm}$ momentum distribution in the rest frame of the $\Upsilon(1S)$. We find evidence for an excess of $D^{*\pm}$ production over the expected rate from the virtual photon annihilation process $\Upsilon(1S) \rightarrow \gamma^* \rightarrow c\bar{c} \rightarrow D^{*\pm}X$.

PACS numbers: 13.25.Gv, 13.87.Fh, 14.65.Dw

*Deceased

†Now at Temple University, Philadelphia, Pennsylvania 19122, USA

‡Also with Università di Perugia, Dipartimento di Fisica, Perugia, Italy

§Also with Università di Roma La Sapienza, I-00185 Roma, Italy

I. INTRODUCTION

Bound states of heavy quarks provide a powerful testing ground for quantum chromodynamics (QCD). Experimental studies of charmonium and bottomonium spectroscopy have helped uncover some of the key aspects of the quarkonium potential [1, 2]. Studies of the decays of quarkonia and of their decay products can also reveal important information on QCD processes [3]. The hadronic decays of the narrow quarkonia, states which are below the threshold for open flavor production, are dominated by couplings to gluons and the fragmentation process into light hadrons. The decay properties of charmonia, which have a relatively low multiplicity particle content, have been extensively studied [4]. However, little is known about the final state contents of bottomonia. In particular, scarcely any experimental information exists on the decays of bottomonium to open charm. The CLEO Collaboration has observed [5] charm production in the decays of the χ_b states with branching fractions of the order of 10%. The ARGUS Collaboration searched [6] for the decay $\Upsilon(1S) \rightarrow D^{*\pm} X$ and set a limit on its branching fraction of $\mathcal{B} < 1.9\%$ at 90% confidence level.

In this article, we report a study of the inclusive process $\Upsilon(1S) \rightarrow D^{*\pm} X$, yielding the decay branching fraction and the $D^{*\pm}$ momentum spectrum in the $\Upsilon(1S)$ rest frame, using data recorded by the BABAR Collaboration at the $\Upsilon(2S)$ resonance. The decay $\Upsilon(1S) \rightarrow D^{*\pm} X$ can proceed through the QED virtual photon annihilation process, $\Upsilon(1S) \rightarrow \gamma^* \rightarrow c\bar{c}$, followed by the hadronization of the $c\bar{c}$ system. The expected decay rate and the $D^{*\pm}$ momentum spectrum from this process can be accurately estimated from the measured properties of the $\Upsilon(1S)$ decays and the charm fragmentation function measured at the center-of-mass energy $\sqrt{s} \sim 10$ GeV. Other QCD processes such as the splitting of a virtual gluon [7–9] or the annihilation of the $b\bar{b}$ system in an octet state [10], have also been suggested as major contributors to this decay channel. Measurements of the $D^{*\pm}$ yield and of its momentum spectrum can help test the predictions of the proposed QCD mechanisms, and possibly reveal the presence of new physics processes with exotic couplings to heavy quarks [11, 12].

II. THE BABAR DETECTOR

The results presented in this work are based on data collected at center-of-mass energy corresponding to the mass of $\Upsilon(2S)$ resonance with the BABAR detector at the PEP-II asymmetric energy e^+e^- storage ring operating at the SLAC National Accelerator Laboratory. The data consist of 14.4 fb^{-1} of integrated luminosity, corresponding to 98.6 ± 0.9 million $\Upsilon(2S)$ mesons produced. The study of $\Upsilon(1S)$ decays is performed by reconstructing the decay chain $\Upsilon(2S) \rightarrow \pi^+\pi^-\Upsilon(1S)$, which yields approximately 17.8 million $\Upsilon(1S)$ decays. An additional off-resonance data sample corresponding to 44.5 fb^{-1} collected at \sqrt{s} about 40 MeV below the $\Upsilon(4S)$ resonance is used to study the background. A GEANT4-based [13] simulation of the detector is used to determine the properties of the signal and to study the background sources.

A detailed description of the BABAR detector can be found elsewhere [14]. The tracking system is composed of a 5 layer silicon vertex tracker (SVT) and a 40 layer drift chamber (DCH) in a 1.5 T magnetic field. The SVT provides a precise determination of the track impact parameters and angles near the interaction point (IP) with $15 \mu\text{m}$ spatial resolution at normal incidence at a radius of 3.2 cm, and is capable of stand-alone tracking for low momentum particles down to $50 \text{ MeV}/c$ of transverse momentum p_t . The DCH, together with the SVT, provides a precise measurement of the momenta and azimuthal angles of charged particles with a resolution $\sigma_{p_t}/p_t = (0.13 p_t \oplus 0.45)\%$, where p_t is in units of GeV/c . Charged hadron identification is achieved through energy measurements of the specific ionization energy loss in the SVT and DCH, and of the Cherenkov angle from a detector of internally reflected Cherenkov light (DIRC). A CsI(Tl) electromagnetic calorimeter (EMC) provides photon detection, electron identification, and π^0 , η and K_L^0 reconstruction. Finally, the instrumented flux return (IFR) of the magnet allows discrimination of muons from pions and detection of neutral kaons.

III. CANDIDATE RECONSTRUCTION AND SELECTION

The $\Upsilon(2S) \rightarrow \pi^+\pi^-\Upsilon(1S)$ candidates are identified by forming pairs of oppositely charged tracks whose recoil mass is consistent with the mass of the $\Upsilon(1S)$ resonance, when the tracks are interpreted as pions. The recoil mass M_{recoil} is computed using

$$M_{\text{recoil}} \equiv \sqrt{(P_{e^+e^-} - P_{\pi\pi})^2} \quad (1)$$

where $P_{e^+e^-}$ is the known 4-momentum of the e^+e^- system and $P_{\pi\pi}$ is the reconstructed 4-momentum of the $\pi^+\pi^-$ pair. The pion tracks are required to have energy losses and Cherenkov angles consistent with the pion hypothesis. The track pair is fitted to a common vertex and the probability of the vertex fit is required to

[¶]Now at University of South Alabama, Mobile, Alabama 36688, USA

**Also with Laboratoire de Physique Nucléaire et de Hautes Energies, IN2P3/CNRS, Université Pierre et Marie Curie-Paris6, Université Denis Diderot-Paris7, F-75252 Paris, France

††Also with Università di Sassari, Sassari, Italy

be greater than 1%. The measured di-pion mass distribution peaks near $0.52 \text{ GeV}/c^2$ for signal events [15], whereas background events are approximately uniformly distributed in the kinematically allowed mass interval $[0.28, 0.56] \text{ GeV}/c^2$. Requiring the mass of the pion pair to be greater than $0.4 \text{ GeV}/c^2$ retains 96% of the signal candidates while rejecting approximately 1/3 of the background events. Figure 1 shows the recoil mass distribution for the event sample passing the above selection criteria; a signal region consisting of two standard deviations around the $\Upsilon(1S)$ mass is highlighted (cross hatching), as well as two sideband regions used for background studies, the lower ($[9432.1, 9444.3] \text{ MeV}/c^2$) and upper ($[9477.7, 9490.0] \text{ MeV}/c^2$) sidebands (diagonal shading). These events form the full event-set used in the measurement of the $D^{*\pm}$ yield.

We reconstruct $D^{*\pm}$ candidates using the decay chain $D^{*+} \rightarrow D^0\pi^+$, $D^0 \rightarrow K^-\pi^+$. A kaon candidate and an oppositely charged pion candidate are combined to form the D^0 candidate. The identification efficiency for kaons (pions) is about 98% (93%); the misidentification rate of kaons (pions) as pions (kaons) is about 5% (15%). The identification performance is obtained from a control sample of inclusive $D^{*+} \rightarrow D^0\pi^+$, $D^0 \rightarrow K^-\pi^+$. The kaon and pion tracks are geometrically constrained to originate from a common vertex and the probability of the vertex fit is required to be greater than 1%. The mass of the D^0 candidate is required to be within $75 \text{ MeV}/c^2$ of the nominal D^0 mass, which corresponds to about 18 times the experimental resolution on the D^0 candidate mass. This large mass interval is necessary for the subtraction of the combinatorial background. The D^0 candidate is finally combined with a soft pion with its charge opposite to that of the kaon candidate to form a D^{*+} candidate. The mass difference between the D^{*+} and the D^0 (Δm) is required to be in the interval $[143.20, 147.64] \text{ MeV}/c^2$, which corresponds to approximately six times the experimental resolution. The soft pion and the D^0 candidates are fitted to a common vertex constrained to originate from the interaction region. The probability of the $D^{*\pm}$ vertex fit is required to be greater than 1%. For events with multiple candidates, the candidate with the best combined vertex fit χ^2 , defined as the sum of the χ^2 values from the vertex fits described above, is kept. The multiplicity of the reconstructed candidates in simulated signal MC events is 1.2, after the final selection. 74% of these candidates are correctly matched to a signal candidate. The best candidate algorithm retains 90% of the correctly matched candidates and 68% of the ones not correctly matched.

IV. SIGNAL EXTRACTION

The sample of $D^{*\pm}$ candidates is studied in intervals of the scaled momentum x_p , defined as:

$$x_p = \frac{p_{D^{*\pm}}}{p_{\max}} \quad (2)$$

where $p_{D^{*\pm}}$ is the $D^{*\pm}$ momentum in the rest frame of the $\Upsilon(1S)$, $p_{\max} = \sqrt{E_{\max}^2 - m_{D^{*+}}^2}$, $E_{\max} = m_{\Upsilon(1S)}/2$ and $m_{D^{*+}}$ is the world average of the D^{*+} mass [16].

The sample is divided into x_p intervals of 0.05 width in the range $[0.1, 1.0]$; the region $x_p < 0.1$, which is dominated by combinatorial background, is excluded.

The invariant mass distribution of the D^0 candidates in each x_p interval is used to determine the $D^{*\pm}$ yield from $\Upsilon(1S) \rightarrow D^{*\pm}X$. The D^0 mass distribution is obtained from the $K^-\pi^+$ candidates mass distribution by two background subtractions. Combinatorial backgrounds, events that are not $\Upsilon(2S) \rightarrow \pi^+\pi^-\Upsilon(1S)$ decays, are removed by subtracting the lower and upper sidebands of the $\pi^+\pi^-$ recoil mass. The $K^-\pi^+$ invariant mass distribution from the sidebands is rescaled to the expected number of background events in the signal region to determine the $K^-\pi^+$ mass distribution from the combinatorial background component under the $\Upsilon(1S)$ peak. In addition, the $K^-\pi^+$ mass distribution for “wrong-sign” $D^0(\rightarrow K^-\pi^+)\pi^-$ combinations (where the soft pion has the same charge as that of the kaon candidate) is used to subtract the D^* combinatoric background including a possible peaking backgrounds from $D^0(\rightarrow K^-\pi^+)\pi^+$ combinations, involving a true D^0 decay and a random soft pion. This method leads to a small over-subtraction of signal events due to doubly Cabibbo suppressed (DCS) D^0 decays reconstructed as wrong-sign combinations. This is accounted for in the final estimation of the branching fraction. The background subtracted invariant mass distribution of D^0 candidates in the full x_p range is shown in Figure 2.

Finally the invariant mass distribution of the D^0 candidates in each x_p interval is fitted to a probability density function (p.d.f.) using a minimum χ^2 estimator. The fitted p.d.f., $P(m)$, is the sum of a signal p.d.f., $P_{\text{sig}}(m)$, and a p.d.f. which accounts for unsubtracted backgrounds, $P_{\text{bkg}}(m)$,

$$P(m) = n_{\text{sig}} \times P_{\text{sig}}(m) + n_{\text{bkg}} \times P_{\text{bkg}}(m) \quad (3)$$

where n_{sig} and n_{bkg} are the number of signal and background events in the fitted region. The fit region corresponds to the D^0 mass range in which we accept signal candidates $[m_{D^0} - 75 \text{ MeV}/c^2, m_{D^0} + 75 \text{ MeV}/c^2]$. The signal p.d.f. is the sum of two Gaussian functions with the same mean:

$$P_{\text{sig}}(m; f, \mu, \sigma_1, \sigma_2) = fG(m; \mu, \sigma_1) + (1 - f)G(m; \mu, \sigma_2) \quad (4)$$

The background p.d.f. is a linear function:

$$P_{\text{bkg}}(m; \mu, p_1) = 1/w + p_1(m - \mu) \quad (5)$$

where w is the fit range. The parameters of the signal p.d.f., σ_1 , σ_2 and f are determined from a fit to the corresponding distribution from Monte Carlo (MC) simulation. However, the mean of the D^0 mass, μ , is fixed to the value determined from a fit to the D^0 mass distribution in the full x_p interval.

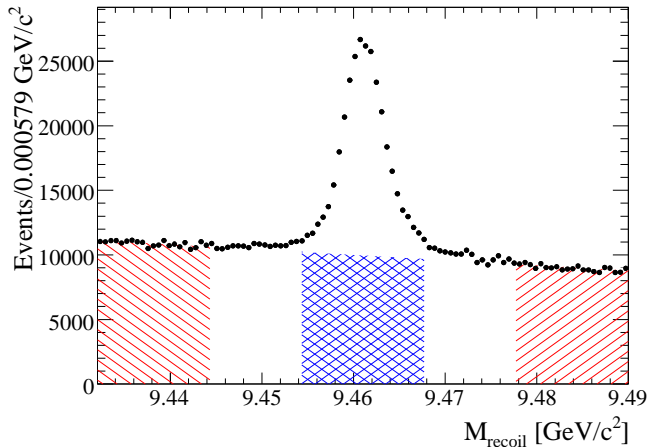


FIG. 1: Distribution of the recoil mass, M_{recoil} , for the selected $\Upsilon(2S) \rightarrow \pi^+\pi^-\Upsilon(1S)$ events. The cross hatching shows the signal region, and the lower and upper sideband regions are indicated by the diagonal shading.

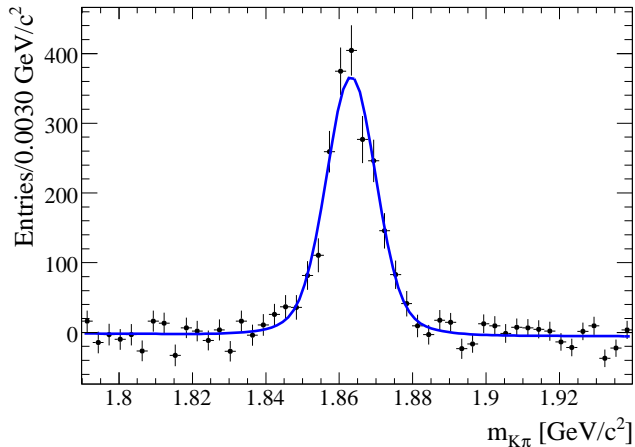


FIG. 2: Distribution of the D^0 invariant mass for the complete $[0.1;1.0]$ x_p range after subtraction of the combinatoric background and wrong-sign combinations. The solid line represents the fit to the data of the p.d.f. described in the text.

The event selection efficiency is determined using a simulation study of the signal and background processes. Signal events are obtained by generating the transition $\Upsilon(2S) \rightarrow \pi^+\pi^-\Upsilon(1S)$ according to the decay model determined by CLEO [15], followed by the decay $\Upsilon(1S) \rightarrow c\bar{c}$ and the hadronization of the $c\bar{c}$ pair via JETSET [17]. Signal events are required to contain at least one $D^{*\pm}$ meson after the hadronization process. The small fraction of events (0.4%) containing both D^{*+} and D^{*-} decays is accounted for by normalizing the efficiency to the number of signal decays generated. The selection efficiency as a function of x_p , $\epsilon(x_p)$, is shown in Figure 3. The dependence on x_p is mainly due to the reconstruction efficiency of the slow pion from the $D^{*\pm}$ decay. The average re-

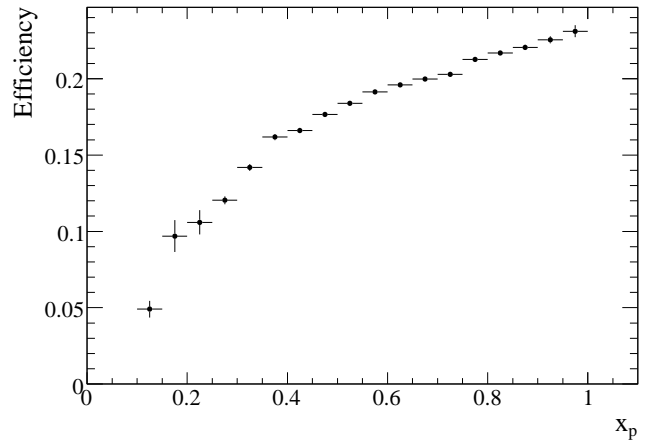


FIG. 3: Reconstruction efficiency for the decay chain $\Upsilon(2S) \rightarrow \pi^+\pi^-\Upsilon(1S)$, $\Upsilon(1S) \rightarrow D^{*\pm}X$ as a function of the scaled $D^{*\pm}$ momentum x_p .

construction efficiency in data depends on the measured x_p distribution and can be estimated from the relation $\langle \epsilon_{\text{data}} \rangle = \frac{\sum_{x_p} n_{\text{sig}}(x_p)}{\sum_{x_p} n_{\text{sig}}(x_p)/\epsilon(x_p)} = (17.7 \pm 0.3)\%$ where the error is statistical only. The ratio of the χ^2 to the number of degrees of freedom for the individual fits ranges from 0.5 to 2.5, with 16 degrees of freedom.

V. RESULTS

Figure 4 shows the efficiency-corrected distribution of the $D^{*\pm}$ yield as a function of x_p . The branching fraction for the inclusive decay $\Upsilon(1S) \rightarrow D^{*\pm}X$ in the x_p range $[0.1, 1.0]$ is computed from:

$$\begin{aligned} \mathcal{B}[\Upsilon(1S) \rightarrow D^{*\pm}X] &= \frac{n_{\text{sig}}}{k_{\text{DCS}} \times \mathcal{B}_{\text{decay}} \times N_{\Upsilon(1S)}} \quad (6) \\ &= (2.52 \pm 0.13(\text{stat}) \pm 0.15(\text{syst}))\% \end{aligned}$$

where $n_{\text{sig}} = \sum_{x_p} n_{\text{sig}}(x_p)/\epsilon(x_p) = 11845 \pm 596$ is the efficiency-corrected signal yield in the x_p range $[0.1, 1.0]$, $k_{\text{DCS}} = (99.62 \pm 0.02)\%$ is a correction factor to account for the subtraction of DCS D^0 decays, $\mathcal{B}_{\text{decay}}$ is the product of the branching fractions [16] in the $D^{*\pm}$ decay chain $\mathcal{B}[D^{*+} \rightarrow D^0\pi^+] = (67.7 \pm 0.5)\%$ and $\mathcal{B}[D^0 \rightarrow K^-\pi^+] = (3.91 \pm 0.05)\%$, $N_{\Upsilon(2S)} = (98.6 \pm 0.9) \times 10^6$, and $N_{\Upsilon(1S)} = N_{\Upsilon(2S)} \times \mathcal{B}[\Upsilon(2S) \rightarrow \pi^+\pi^-\Upsilon(1S)] = (17.8 \pm 0.4) \times 10^6$ is the number of $\Upsilon(1S)$ mesons produced in this decay chain.

We verify that our analysis procedure is unbiased by fitting off-resonance data and a Monte Carlo simulation of the background; we find no significant signal. We also compare the lower and upper sidebands and use the D^0 mass sidebands instead of the recoil mass to subtract the background, and we find no significant shift in the signal. The sources of systematic uncertainty are listed in

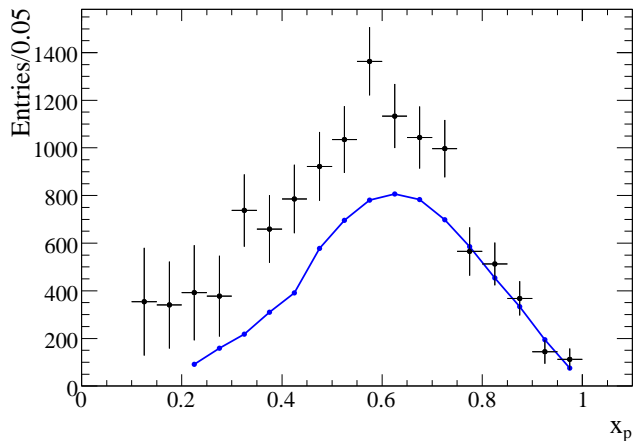


FIG. 4: Signal yield as a function of x_p . The solid line represents the expected contribution from the virtual photon process [18].

TABLE I: Summary of the systematic uncertainties on $\mathcal{B}[\Upsilon(1S) \rightarrow D^{*\pm}X]$.

Sources of systematic uncertainty	Relative uncertainty
Slow π^\pm reconstruction efficiency	3.0%
M_{recoil} selection	2.8%
$\mathcal{B}_{\text{decay}} \times \mathcal{B}[\Upsilon(2S) \rightarrow \pi^+\pi^-\Upsilon(1S)]$	2.3%
Generated x_p distribution	2.2%
PID	1.6%
Tracking efficiency (excl. slow pion)	1.6%
$\Upsilon(2S)$ decay model	1.2%
Υ counting	0.9%
Background curvature	0.4%
MC efficiency	0.4%
Signal shape	0.3%
k_{DCS}	0.02%
Total systematic uncertainty	5.9%

Table I. The main contributions come from the uncertainties in the knowledge of the slow pion reconstruction efficiency and the selection efficiency of $\Upsilon(1S)$ decays in the recoil mass signal region. The former is determined from a control sample of $D^{*+} \rightarrow D^0\pi^+$ decays by comparing the efficiency in data with that in MC events, for the soft pion momentum range [50, 400] MeV. The efficiency is extracted from a study of the angular distribution of the soft pion in the rest frame of the D^* meson. The M_{recoil} selection systematic uncertainty is obtained by comparing the recoil mass distribution for signal events in the full x_p range [0.1, 1.0] in data, with the distribution in Monte Carlo simulated events. The fit to data with the sum of two Gauss functions gives an r.m.s. of 2.9 MeV while the fit to MC events gives 3.3 MeV. The efficiency is estimated from the integral of the fitted function in a window around the $\Upsilon(1S)$ mass of $\pm 2 \times$ the r.m.s. on MC (the recoil mass signal region). The efficiency in data is 96.3% while in MC events is

93.6%, which corresponds to a relative systematic error on the result of 2.8%. The uncertainty associated with the generated x_p distribution is determined by reweighting simulated signal MC events according to the x_p distribution measured using data. In addition the parameters of the $\Upsilon(2S)$ decay model have been varied within their uncertainty and the resulting relative efficiency variation has been taken as the systematic uncertainty. The uncertainty in the particle identification efficiency (PID) is derived from a study of a $\phi \rightarrow K^+K^-$ control sample and by removing the PID requirement from the selection. The dominant systematic uncertainties in the Υ counting come from the modeling of the track reconstruction efficiency and of the total energy of the events. The signal shape uncertainty is due to data-MC differences in the D^0 mass signal distribution. A possible curvature of the background is extracted from off-resonance data, and the systematic uncertainty is obtained by adding the corresponding second order polynomial to the background p.d.f.. The uncertainties due to MC efficiency, k_{DCS} and $\mathcal{B}_{\text{decay}} \times \mathcal{B}[\Upsilon(2S) \rightarrow \pi^+\pi^-\Upsilon(1S)]$ arise from imperfect knowledge of these parameters.

VI. DISCUSSION AND CONCLUSION

Figure 4 shows the expected x_p distribution for $D^{*\pm}$ production from the QED virtual photon annihilation process, $\Upsilon(1S) \rightarrow \gamma^* \rightarrow c\bar{c}$. The shape is obtained from the measured $D^{*\pm}$ fragmentation function at $\sqrt{s} = 10.5$ GeV [18] and the normalization is computed from:

$$\mathcal{B}[\Upsilon(1S) \rightarrow \gamma^* \rightarrow D^{*\pm}X] = \frac{\sigma_{D^{*\pm}}}{\sigma_{q\bar{q}}} \times R_{\text{had}} \quad (7)$$

$$\times \mathcal{B}[\Upsilon(1S) \rightarrow \mu^+\mu^-]$$

where, $R_{\text{had}} = \sigma(e^+e^- \rightarrow \text{hadrons})/\sigma(e^+e^- \rightarrow \mu^+\mu^-) = 3.46 \pm 0.13$ [19], $\mathcal{B}[\Upsilon(1S) \rightarrow \mu^+\mu^-] = (2.48 \pm 0.05)\%$ [16], and $\frac{\sigma_{D^{*\pm}}}{\sigma_{q\bar{q}}} = (17.7 \pm 2.2)\%$ [16] is the measured $D^{*\pm}$ yield from $e^+e^- \rightarrow q\bar{q}$ at $\sqrt{s} = 10.5$ GeV. We find $\mathcal{B}[\Upsilon(1S) \rightarrow \gamma^* \rightarrow D^{*\pm}X] = (1.52 \pm 0.20)\%$.

Our measured branching fraction exceeds the expected rate from the QED virtual photon process from Eq. 7 by $(1.00 \pm 0.28)\%$ (including the systematic uncertainty) which corresponds to 3.6 standard deviations. While the measured x_p spectrum agrees in shape with that of the virtual photon process for $x_p > 0.75$, there is a significant excess for $x_p < 0.75$. The probability that the measured spectrum is consistent with the expected distribution from the virtual photon, normalized using Eq. (7), is 1.2×10^{-5} confidence estimated from a binned χ^2 test. The excess is compatible with the contribution expected [9] from the splitting of a virtual gluon, $(1.20 \pm 0.29)\%$. This does not leave much room for the octet contribution [10], which is also disfavored from the shape of the excess as a function of x_p .

In summary, using the data collected with the *BABAR* detector at the $\Upsilon(2S)$ resonance, we have observed for

the first time the decay of $\Upsilon(1S)$ mesons to open charm. We have measured the branching fraction $\mathcal{B}[\Upsilon(1S) \rightarrow D^{*\pm} X] = (2.52 \pm 0.13(\text{stat}) \pm 0.15(\text{syst}))\%$ and the $D^{*\pm}$ momentum distribution in the rest frame of the $\Upsilon(1S)$. We find evidence for a significant excess of $D^{*\pm}$ production with respect to the expectation from the virtual photon annihilation process.

Acknowledgments

We are grateful for the extraordinary contributions of our PEP-II colleagues in achieving the excellent luminosity and machine conditions that have made this work possible. The success of this project also relies critically on the expertise and dedication of the computing organizations that support *BABAR*. The collaborating institutions

wish to thank SLAC for its support and the kind hospitality extended to them. This work is supported by the US Department of Energy and National Science Foundation, the Natural Sciences and Engineering Research Council (Canada), the Commissariat à l’Energie Atomique and Institut National de Physique Nucléaire et de Physique des Particules (France), the Bundesministerium für Bildung und Forschung and Deutsche Forschungsgemeinschaft (Germany), the Istituto Nazionale di Fisica Nucleare (Italy), the Foundation for Fundamental Research on Matter (The Netherlands), the Research Council of Norway, the Ministry of Education and Science of the Russian Federation, Ministerio de Educación y Ciencia (Spain), and the Science and Technology Facilities Council (United Kingdom). Individuals have received support from the Marie-Curie IEF program (European Union) and the A. P. Sloan Foundation.

-
- [1] E. Eichten *et al.*, Phys. Rev. Lett. **34**, 369 (1975).
 [2] J. L. Rosner, J. Phys. Conf. Ser. **69**, 012002 (2007).
 [3] E. Eichten, S. Godfrey, H. Mahlke, and J. L. Rosner, Rev. Mod. Phys. **80**, 1161 (2008).
 [4] N. Brambilla *et al.* (Quarkonium Working Group), CERN Yellow Report **CERN-2005-005** (2005).
 [5] R. A. Briere *et al.* (CLEO), Phys. Rev. **D78**, 092007 (2008).
 [6] H. Albrecht *et al.* (ARGUS), Z. Phys. **C55**, 25 (1992).
 [7] H. Fritzsche and K. H. Streng, Phys. Lett. **B77**, 299 (1978).
 [8] I. I. Y. Bigi and S. Nussinov, Phys. Lett. **B82**, 281 (1979).
 [9] D. Kang, T. Kim, J. Lee, and C. Yu, Phys. Rev. **D76**, 114018 (2007).
 [10] Y.-J. Zhang and K.-T. Chao, Phys. Rev. **D78**, 094017 (2008).
 [11] R. Dermisek, J. F. Gunion, and B. McElrath, Phys. Rev. **D76**, 051105 (2007).
 [12] B. Bellazzini *et al.* (2009), arXiv:0910.3210v1.
 [13] S. Agostinelli *et al.* (GEANT4), Nucl. Instrum. Meth. **A506**, 250 (2003).
 [14] B. Aubert *et al.* (*BABAR*), Nucl. Instrum. Meth. **A479**, 1 (2002).
 [15] D. Cronin-Hennessy *et al.* (CLEO), Phys. Rev. **D76**, 072001 (2007).
 [16] C. Amsler *et al.* (Particle Data Group), Phys. Lett. **B667**, 1 (2008).
 [17] T. Sjostrand, Comput. Phys. Commun. **82**, 74 (1994).
 [18] M. Artuso *et al.* (CLEO), Phys. Rev. **D70**, 112001 (2004).
 [19] H. Albrecht *et al.* (ARGUS), Z. Phys. **C54**, 13 (1992).